

## Article

# Environment-Friendly Corrosion Inhibitors for Aluminum in Hydrochloric Acid: Quantum and Experimental Research

Tarek A. Yousef <sup>1,2</sup>, Rageh. K. Hussein <sup>3</sup>, Abdulrahman G. Alhamzani <sup>1,\*</sup>, Ahmed T. Al-Enazi <sup>1</sup>,  
Mohammed B. AL-Osimi <sup>1</sup> and Mortaga M. Abou-Krishna <sup>1,4</sup>

<sup>1</sup> Chemistry Department, College of Science, Imam Mohammad Ibn Saud Islamic University (IMSIU), Riyadh 11623, Saudi Arabia

<sup>2</sup> Mansoura Laboratory, Department of Toxic and Narcotic Drug, Forensic Medicine, Medicolegal Organization, Ministry of Justice, Mansoura 35511, Egypt

<sup>3</sup> Physics Department, College of Science, Imam Mohammad Ibn Saud Islamic University (IMSIU), Riyadh 11623, Saudi Arabia

<sup>4</sup> Department of Chemistry, South Valley University, Qena 83523, Egypt

\* Correspondence: agalhamzani@imamu.edu.sa

**Abstract:** Environment-friendly materials (e.g., Honey and Mint) are used as corrosion inhibitors for aluminum in hydrochloric acid (HCl) using both the density functional theory (DFT) at the B3LYP/6–31G\* basis set level and semi-empirical methods (AM1, PM3, MINDO, and RM1). The aim of this study is to investigate the inhibition efficiency (%IE) in terms of their molecular structure. The quantum chemical parameters such as the highest occupied molecular orbital energy ( $E_{\text{HOMO}}$ ), the lowest unoccupied molecular orbital energy ( $E_{\text{LUMO}}$ ), the energy gap ( $\Delta E$ ), the charge on the reactive core, the hardness ( $\eta$ ), and the total energy have all been computed. The MINDO method was used to measure the electronic energies and charge densities of the inhibitors that were used. Theoretical calculations were also carried out, with the findings correlating well with the experimental data. Gravimetry and gasometry measurements were used to investigate the effects of honey and mint on aluminum corrosion in a 1.0 M hydrochloric acid (HCl) solution. In acid solutions, honey and mint were found to be effective inhibitors of aluminum corrosion, with honey being the better option. Because of the adsorption of its components on aluminum surfaces, the inhibitory effect of the used inhibitors was addressed. The higher dipole moment of honey than that of mint caused the adsorption of honey on the aluminum surface better. The IEs measured by gravimetry and gasometry are almost identical.

**Keywords:** density functional theory (DFT); semi-empirical methods; honey; mint; aluminum corrosion; gravimetry; gasometry



**Citation:** Yousef, T.A.; Hussein, R.K.; Alhamzani, A.G.; Al-Enazi, A.T.; AL-Osimi, M.B.; Abou-Krishna, M.M. Environment-Friendly Corrosion Inhibitors for Aluminum in Hydrochloric Acid: Quantum and Experimental Research. *Metals* **2022**, *12*, 1538. <https://doi.org/10.3390/met12091538>

Academic Editors: Frank Czerwinski and Alexandre Emelyanenko

Received: 8 August 2022

Accepted: 14 September 2022

Published: 17 September 2022

**Publisher's Note:** MDPI stays neutral with regard to jurisdictional claims in published maps and institutional affiliations.



**Copyright:** © 2022 by the authors. Licensee MDPI, Basel, Switzerland. This article is an open access article distributed under the terms and conditions of the Creative Commons Attribution (CC BY) license (<https://creativecommons.org/licenses/by/4.0/>).

## 1. Introduction

Corrosion is a natural phenomenon that degrades the properties of metals and alloys, rendering them unusable, and it may be chemical or electrochemical in nature. Aluminum is a nonmagnetic and non-sparkling smooth, tough, lightweight, malleable metal with a silvery to dull grey appearance based on surface roughness. Aluminum and its alloys can be used in construction and interior fittings, as well as in several industries and hazardous environments. Aluminum is known for its low density and ability to resist corrosion to some extent due to passivation; however, it corrodes in aqueous acidic environments. In acid solutions, aluminum and its alloys' corrosion have been extensively investigated [1–3]. In the industry, certain compounds are used as corrosion inhibitors to deter or slow the corrosion of metals in acidic environments. Because of the toxicity and high cost of these compounds, it is important to find friendlier and less costly inhibitors.

Because of growing environmental consciousness and tighter environmental laws governing the use of man-made corrosion inhibitors, the search for environmentally sus-

tainable substitutes, also known as green corrosion inhibitors, has begun [4]. Natural plant-based products [5,6] and non-toxic man-made chemicals such as dyes [7–9], rare earth elements [10,11], Schiff bases [12–14], and certain drugs [15,16] can be used as environmentally safe corrosion inhibitors. For nearly two decades, scientists have been conducting extensive research to produce new forms of non-toxic aluminum corrosion inhibitors [17]. The process of green corrosion inhibition in aluminum and its alloys in alkaline aqueous conditions has been the subject of numerous theories. Green corrosion inhibitors are thought to slow aluminum corrosion by increasing the pH stability spectrum of amphoteric layers made up of aluminum oxides and hydroxides and/or repairing/rebuilding weakened oxide and hydroxide layers, reducing reactive reagent diffusion speeds to and from the metal's surface and/or eliminating corrosion products from the metal's surface [18].

Bee products have been described as effective green corrosion inhibitors for aluminum and its alloys. The anti-corrosive effects of natural honey in seawater, when exposed to Al-Mg-Si alloy, were investigated by Rosliza et al. [19]. The presence of a thin layer of corrosion inhibitor on the protected alloy's surface was confirmed by SEM analysis; this layer reduced the overall rate of corrosion. Gudic et al. [20] reported similar findings.

Natural products from tannin-rich plant extracts [21–23], black pepper extract [24], mint [25], Lawsonia [26], and Opuntia extract [2], as well as extracts from different parts of the plant such as leaves [27] and roots [28], are environmentally safe, non-toxic and comparatively less costly. Bedair et al. [25] investigated the effect of certain natural ingredients such as mint stems and leaves on mild steel corrosion in 1.0 M HCl. They concluded that the plant extracts were mixed-type inhibitors. By increasing their concentrations and lowering the temperature of the atmosphere, these compounds' inhibition efficiencies (IEs) improved.

Experiments are useful for explaining inhibition mechanisms, but they can be costly and time-consuming. Many research and industrial labs now have access to high-performance computing and graphical resources thanks to the advancements in computer hardware and software and theoretical chemistry. More recent papers concerning the topic of corrosion [29,30] have included significant quantum chemical measurements. These calculations are commonly used to investigate the inhibitors' electronic properties.

Several papers reported using honey or mint as a corrosion inhibitor; however, there is little or no literature on numerical modeling of molecular structure characteristics of honey- and mint-friendly inhibitors as aluminum corrosion inhibitors in HCl. Thus, for this study, the authors focused their efforts on evaluating honey and mint as aluminum corrosion inhibitors in HCl, using molecular structure numerical simulations and then theoretically verifying using very simple methods, gravimetric and gasometric methods.

## 2. Experimental Section

### 2.1. Computational Methods and Details

Geometric optimizations of atoms were carried out using the Density Functional Theory (DFT) at B3LYP formalism with an electron base set 6–31G (d,p). Quantum chemical calculations were also performed using the widely used Gaussian-03 software package (03, Gaussian, Wallingford, CT, USA) [31]. Measurements of the energy of the highest occupied molecular orbital (EHOMO), the energy of the lowest unoccupied molecular orbital (ELUMO), the energy gap ( $\Delta E$ ), and the dipole moment have been performed to understand the inhibition mechanisms with regard to the molecular structures. The HyperChem series of programs force field, which was introduced in HyperChem 8.0 (v8.0, Hypercube Inc., Cambridge, ON, Canada), was used to carry out semi-empirical computations using the AM1, PM3, MNDO, and RM1 semi-empirical methods [32].

Al (111), which has more active sites and a larger surface atom coordination number than other surfaces [33], was chosen as the adsorption substrate for MC modeling in this study. The Adsorption Locator module's MC simulation was used to examine the adsorption of honey, mint, and water on Al (111). The adsorption model had a dimension of  $40.49 \text{ \AA} \times 28.63 \text{ \AA} \times 21.43 \text{ \AA}$  and was made up of six layers of Al (111) atoms and 25 layers

of vacuum. The COMPASS [34] forcefield was used to optimize the adsorption structures. The Ewald approach and the atom-based method were selected as the electrostatic and van der Waals summation methods, respectively. The Ewald method's precision was adjusted at  $1 \times 10^{-4}$  Kcal mol<sup>-1</sup>. The atom-based method's cutoff distance and spline width were set to 15.5 Å and 1 Å, respectively.

## 2.2. Aluminum Specimens and Reagents

The specimens used in this investigation were made from 99.99% pure aluminum, in a rectangular shape having 4 cm × 1.3 cm × 0.13 cm. They were used for the gravimetric process. The aluminum samples, for the gasometry method, were having 3 cm × 0.6 cm × 0.13 cm. A prepared solution of Na<sub>2</sub>CO<sub>3</sub> (25 g/L), Na<sub>3</sub>PO<sub>4</sub> (25 g/L), and a wetting agent (a synthetic detergent with the active ingredient dodecylbenzene sulphonate) (10 g/L) was used to degrease the aluminum specimens at 85.0 °C for 2 min, and subsequently washed with distilled water. Then, the samples were dipped in a pickling solution of 4 M HCl for one minute, followed by washing with hot and cold water.

Honey and mint contain different ingredients, so the authors suggest choosing the key component, sucrose for honey and menthol for mint, for the theoretical analysis, which is depicted in Figure 1.

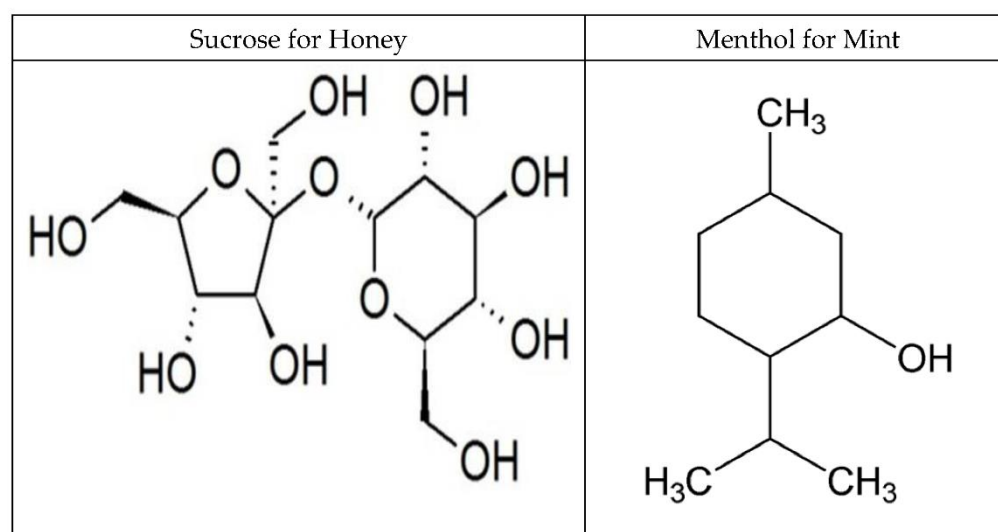


**Figure 1.** Molecular structures of the main ingredients of honey and mint as the inhibitors employed in the experiment.

## 2.3. Preparation of Solutions

The corrosive aqueous solution was made with an analytical grade 37% HCl solution from Merck Chemicals. Natural honey's chemical composition varies slightly depending on the type. Clover honey was included in the current research. The concentration of the stock solution was measured in parts per million (ppm) using double distilled water as the stock solution.

Mint leaves (*Mentha Pulegium*) were dried at 60 °C to a constant weight and ground into powder to extract the mint inhibitor. To completely immerse the mint powder, an adequate quantity of powder is put in a flask, followed by enough distilled water. After 3 h of refluxing, the mixture was filtered. The filtrate was evaporated and concentrated to obtain the crude powder, which was then dried in an electric oven to obtain the mint extract. The rigid material was removed and crushed into powder once more. With double distilled water as the stock solution, the concentration of the stock solution was expressed in terms of ppm.

The corrosive solution was made by diluting a commercial HCL solution with doubly distilled water (blank was a 1 M HCl). Inhibitor-containing 1 M HCl solutions were prepared with concentrations ranging from 300 to 900 ppm.

#### 2.4. Gravimetric Measurements

In a 100-mL and a 50-mL beaker of the test solution, gravimetric measurements were performed. The immersion time for weight loss was 2 h at 298 K. To acquire good reproducible data, parallel triplicate tests were correctly completed and used to compute the corrosion rates (CRs).

The following equation, Equation (1), is used to compute CRs:

$$\text{Corrosion Rates} = \frac{WL}{(A_s \times t)} \quad (1)$$

where  $WL$  is the weight loss in milligrams,  $A_s$  is the sample surface areas in  $\text{cm}^2$ , and  $t$  is the immersion time in hours. Equation (2) was used to compute the inhibition efficiency, %IE:

$$\%IE = \frac{CR_0 - CR_i}{CR_0} \times 100 \quad (2)$$

where  $CR_0$  is the rate of corrosion of aluminum specimen in the blank solution (i.e., HCl solution without inhibitors) in  $\text{mg cm}^{-2} \text{h}^{-1}$ , and  $CR_i$  is the rate of corrosion of aluminum specimen in HCl solution with a certain amount of inhibitor in  $\text{mg cm}^{-2} \text{h}^{-1}$ . Equation (3) shows the degree of surface covering ( $\theta$ ), and IE can be written as follows:

$$\theta = \frac{CR_0 - CR_i}{CR_0} \quad (3)$$

#### 2.5. Gasometric Measurements

The volumetric measurement of evolved hydrogen was used to track the development of the corrosion reaction. The corrosion rate,  $CR$ , in  $\text{mL min}^{-1}$  was calculated using the slope of a straight line, illustrating the variability in hydrogen volume and exposure time. The following equation, i.e., Equation (4), was used to calculate the IE:

$$\%IE = \left(1 - \frac{CR}{CR_0}\right) \times 100 \quad (4)$$

where  $CR$  and  $CR_0$  are the CRs, in which the  $CR$  is the rate of corrosion of aluminum specimens in the presence of inhibitors, and  $CR_0$  is the rate of corrosion of specimens in the absence of the used inhibitors.

#### 2.6. Adsorption Isotherm

The adsorption isotherm model may be derived by assuming that the inhibitory effect is primarily due to the adsorption at metal/solution contact [35]. Adsorption isotherms can provide basic information about the adsorption of inhibitor on the metal surfaces. The isotherm may be driven by the determination of the fractional surface coverage data ( $\theta$ ) as a function of inhibitor concentration. Hence, empirically determining which isotherm best suits the adsorption of inhibitor on the aluminum surface is required. The Freundlich isotherm model describes the experimental data for surfaces coverage, as illustrated in the following equation:

$$\log\theta = \log K + \frac{1}{n} \log C \quad (5)$$

Langmuir isotherm model is another model that can be applied to test the adsorption isotherm, as shown in Equation (6):

$$\frac{C}{\theta} = \frac{1}{K} + n C \quad (6)$$

A plot of  $C/\theta$  versus the concentration,  $C$ , gives the values of the constants,  $K$  and  $n$ .

### 2.7. Surface Characterization

Scanning electron microscope (SEM) images of the aluminium surfaces were obtained using the JSM-5500 LV Scanning Electron Microscope (JEOL Ltd., Tokyo, Japan) The morphology of the aluminium surfaces was examined after immersion in HCl (i.e., in the presence and absence of the inhibitor) for one hour at ambient room temperature.

## 3. Results and Discussion

### 3.1. Quantum Chemical Calculations

Quantum chemical simulations were used to investigate the effect of molecule structure on inhibitory behavior [36]. The extent of interaction between the active sites of inhibitor molecules and the aluminum surface was calculated using DFT [37]. Recently, corrosion mechanisms have been thoroughly assessed using both electrochemical and computational modeling methods [38,39]. Figure 2 illustrates the optimal molecular structure of these molecules. Additionally, frontier molecule orbital density distributions of these compounds are depicted in Figure 3.

Quantum chemical characteristics, such as  $E_{\text{HOMO}}$ ,  $E_{\text{LUMO}}$ ,  $E_{\text{LUMO}}-E_{\text{HOMO}}$  (energy gap  $E$ ), dipole moment ( $\mu$ ), and electronegativity, have been obtained, and they are presented in Table 1. The value of  $E_{\text{HOMO}}$  is connected to a molecule's ability to donate electrons to appropriate electron acceptors, according to the frontier molecular orbital theory. The value of  $E_{\text{LUMO}}$ , on the other hand, is proportional to the molecule's ability to receive electrons [40–42]. A molecule with a higher  $E_{\text{HOMO}}$  value and/or lower  $E_{\text{LUMO}}$  value tend to have a higher %IE [43–46]. From Table 1, we can understand that all the calculated values of  $E_{\text{HOMO}}$  and  $E_{\text{LUMO}}$  strongly adhere to the following order: honey > mint, which matches well with that of the IE. Another useful parameter, dipole moment ( $\mu$ ), can be used to see the connection between the inhabitation and molecular structure of the inhibitor. In general, the higher value of  $\mu$  reveals that the adsorption of the molecule into the metal surface is strong, and results in a higher value of IE [46,47]. We can see in Table 1 that the dipole moment of these two compounds is consistent with the order: honey is greater than the mint except for PM3 and RM1 methods, which explains the priority of honey over mint in inhibitory properties.

Based on literature, the correlation between the dipole moment and the inhibition efficiency is still under discussion [48,49]. Some researchers have reported that lower dipole moment values reveal a good inhibition effect [50,51]. On the other hand, chemical potential can be determined by values of electronegativity, as they indicate the freedom of electrons on the inhibitors. However, higher electronegativities indicate better inhibition. From the obtained data in Table 1, honey showed higher values of electronegativity.

Local electron densities or charges have been shown to play a role in many chemical processes and physiochemical characteristics of substances [52]. Adsorption on a metal surface explains the inhibition action of organic compounds because aluminum's surface is positively charged in an acidic solution [53]. Table 2 shows that all the oxygen atoms in honey and mint have negative charges, indicating that these atoms are negative charge centers, capable of offering electrons to the aluminum surface and forming a coordination kind of link.

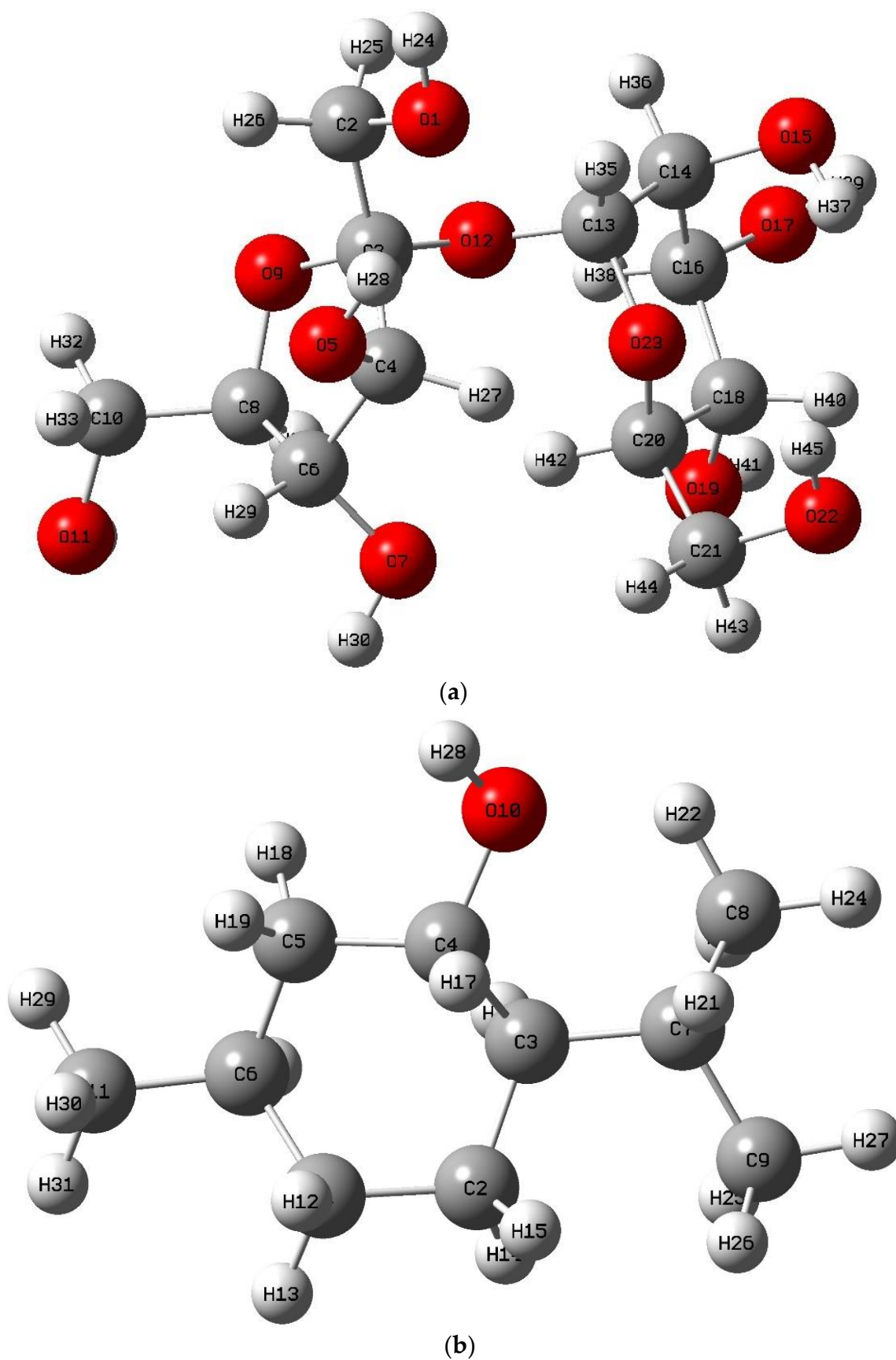


Figure 2. Optimized structure of (a) Honey and (b) Mint using B3LYP/6-31G\*(d,p).

Another essential factor to examine in terms of energy levels is the difference between the HOMO and LUMO energies for the molecules under study. Cherry et al. [54] exploited the  $E_{\text{LUMO}}-E_{\text{HOMO}}$  concept to construct theoretical models capable of qualitatively understanding the structural and conformation barriers in many molecular systems. Low absolute values of the energy gap ( $\Delta E$ ) result in high IE because the energy required to remove an electron from the final occupied orbital is very small [55]. According to the data in Table 1, the AM1 method provides a strong correlation in the  $E_{\text{LUMO}}-E_{\text{HOMO}}$ . Honey is the best inhibitor and has the shortest  $E_{\text{LUMO}}-E_{\text{HOMO}}$  (i.e., 12.192 eV), whereas mint is the least inhibitor and has the largest  $E_{\text{LUMO}}-E_{\text{HOMO}}$  (i.e., 13.676 eV). The inhibition rose to 4.1% because of the 1.484 eV difference between the energy gap of honey and the mint. Table 1 shows that, as the  $\Delta E$  values decline, the IE increases, indicating the stability of created complexes between honey, mint, and aluminum i.e., the order of IEs is as follows: As evidenced by experimental data, honey outperforms mint. This means that the best correlations between experimental and IEs obtained were achieved using DFT and semi-empirical approaches for gaseous phase. According to the literature, when correlation coefficients is greater than 60% in corrosion investigation, it highly appreciated in quantum chemical calculations [55]. Honey has a higher IE than mint because it contains more oxygen atoms. Honey has an abundance of unbound lone pair electrons that can bond with aluminum. DFT was used to calculate the protonated forms of both Honey and Mint at the B3LYP/6-31G\* level, which is the same level used to calculate the neutral (non-protonated) type. The energy gaps of Honey and Mint in their protonated forms are considerably smaller than the neutral form. The dipole moment value has increased in the protonated form, resulting in improved organic molecule adsorption to metal surfaces. The inhibitors exhibited more softness and less hardness in the protonated state. These results imply that, in a protonated form, the inhibitors have higher reactivity.

The molecular structure of an inhibitor affects its adsorption efficiency. The presence of rigidity of a  $\pi$ -delocalized system, more donor functional groups and substituents on benzene rings may result in an increase in electron density at the adsorption center, which produces more coordinate bonding and easier electron transfer to the metal, leading to higher inhibition efficiency. Honey has a higher IE than mint because it contains more oxygen atoms. Honey has an abundance of unbound lone pair electrons that can bond with aluminum. The results demonstrate a good agreement between the computational calculations and the experimental data [37].

The stability and reactivity of a compound could also be used to evaluate its hardness and softness. Thus, compounds are highly reactive compared to hard compounds, and they effortlessly provide electrons to an Al sample during the adsorption. Thus, they work as effective corrosion inhibitors [56]. As shown in Table 1, Honey has an average  $s$  value (3.18), while Mint has an average  $s$  value (3.48) with values that are very close to each other, which demonstrates the small differences in inhibition efficiency. The same explanation also goes for the case of hardness.

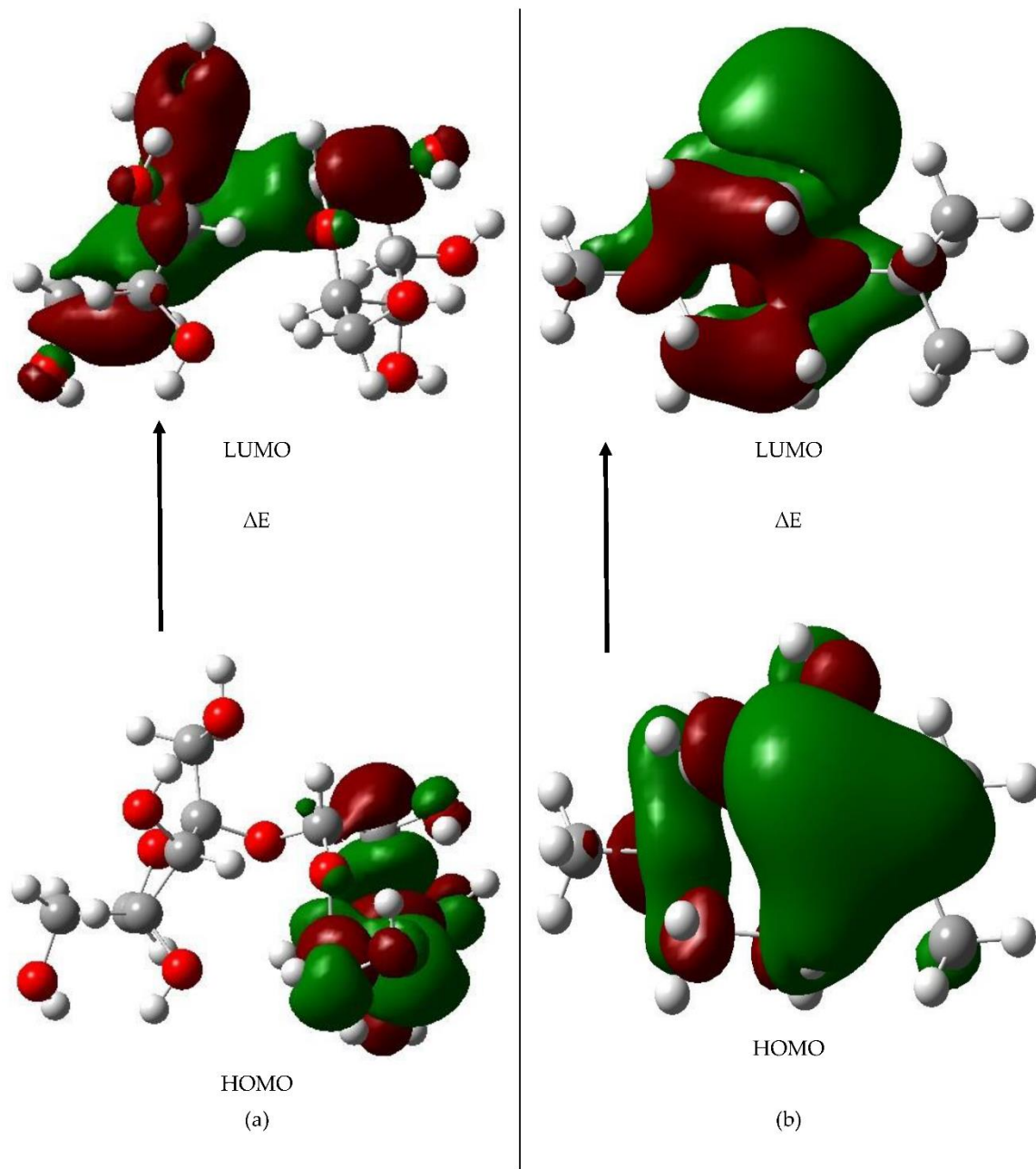


Figure 3. Plots of frontier orbitals and energy gap for (a) Honey and (b) Mint.

**Table 1.** Gas-phase AM1, MNDO, PM3, RM1, and B3LYP/6-31G\*(d,p) data for honey and mint.

Method	Inhibitor	$E_{\text{HOMO}}$	$E_{\text{LUMO}}$	$\Delta E$	Hardness	Softness	Chemical Potential	Electrophilicity Index	Dipole-Moment	Electro-Negativity	% Inhibition
AM1	Honey	-10.54	1.64	12.19	6.09	3.05	-4.45	1.63	3.59	4.45	89.3
MINDO		-10.52	2.31	12.83	6.42	3.21	-4.11	1.31	2.14	4.11	89.3
PM3		-10.78	1.76	12.54	6.27	3.14	-4.51	1.62	0	4.51	89.3
RM1		-10.44	2.16	12.6	6.3	3.15	-4.14	1.36	0	4.14	89.3
B3LYP/6-31G*(d,p)		-11.04	2.5	13.54	6.77	3.39	-4.27	1.35	3.69	4.27	89.3
B3LYP/6-31G*(d,p) protonated form		-6.83	0.96	7.79			3.82				
AM1	Mint	-10.45	3.21	13.67	6.83	3.42	-3.62	6.83	1.54	3.62	85.2
MINDO		-10.98	2.88	13.86	6.93	3.47	-4.05	6.93	1.32	4.05	85.2
PM3		-10.88	3.02	13.91	6.95	3.48	-3.93	6.95	1.41	3.93	85.2
RM1		-10.47	3.37	13.84	6.92	3.46	-3.55	6.92	1.45	3.55	85.2
B3LYP/6-31G*(d,p)		-11.39	2.98	13.57	7.19	3.59	-4.21	7.19	2.12	4.21	85.2
B3LYP/6-31G*(d,p) protonated form		-6.73	2.03	8.76			2.76				

**Table 2.** Mulliken atomic charges of honey and mint by B3LYP/6-31G\*.

Honey			Mint		
1	O	−0.350	1	C	−0.155
2	C	−0.036	2	C	−0.154
3	C	0.176	3	C	−0.090
4	C	−0.001	4	C	0.034
5	O	−0.320	5	C	−0.190
6	C	0.012	6	C	−0.099
7	O	−0.319	7	C	−0.092
8	C	−0.042	8	C	−0.209
9	O	−0.249	9	C	−0.209
10	C	−0.028	10	O	−0.326
11	O	−0.324	11	O	−0.208
12	O	−0.304			
13	C	0.121			
14	C	−0.016			
15	O	−0.320			
16	C	−0.037			
17	O	−0.322			
18	C	−0.023			
19	O	−0.319			
20	C	−0.003			
21	C	−0.014			
22	O	−0.326			
23	O	−0.316			

### 3.2. MC Simulations

The strength and arrangement of the adsorption on the metal surface have a direct impact on how well organic corrosion inhibitor molecules block corrosion [57]. The most stable arrangement of organic molecules adsorbed on the metal surface may be precisely determined using MC modeling, and the adsorption energy can be calculated [58]. In MC simulations [22], the rigid adsorption energy and the deformation energy are added to determine the adsorbed substance's adsorption energy. While the deformation energy refers to the energy released or required when the adsorbates are relaxed, the stiff adsorption energy refers to the energy released or necessary when unrelaxed adsorbates adsorb on the substrate. MC simulations were used to perceive the interactions between the honey, mint and the Al surface and the mechanism of adsorption. Figure 4 shows the most likely adsorption configurations for honey and mint on the Al sample. This was achieved by the adsorption locator module that presents the smooth disposition and suggests an improvement in the adsorption with the highest surface coverage. Table 3 also compiles the results of the Monte Carlo simulations' calculations. In the table, rigid adsorption energies for unrelaxed adsorbate compounds, relaxed adsorbate compound deformation energies, and adsorption energies for relaxed adsorbate compounds are all listed. Compared to Honey ( $-9570.46 \text{ kcal mol}^{-1}$ ), Mint displayed a lower result for adsorption energy ( $9114.16 \text{ kcal mol}^{-1}$ ). This demonstrated the Honey's increased ability to bind to the surface of Al, creating a stable adsorbed barrier that inhibits corrosion. These findings are consistent with the experimental data. The values for the adsorption energy for Honey at the unrelaxed and relaxed stages of geometry optimization were  $-235.35$  and  $956.81 \text{ kcal mol}^{-1}$ , respectively.

These values were more negative for Honey than for Mint, indicating a stronger propensity toward prohibition for Honey.

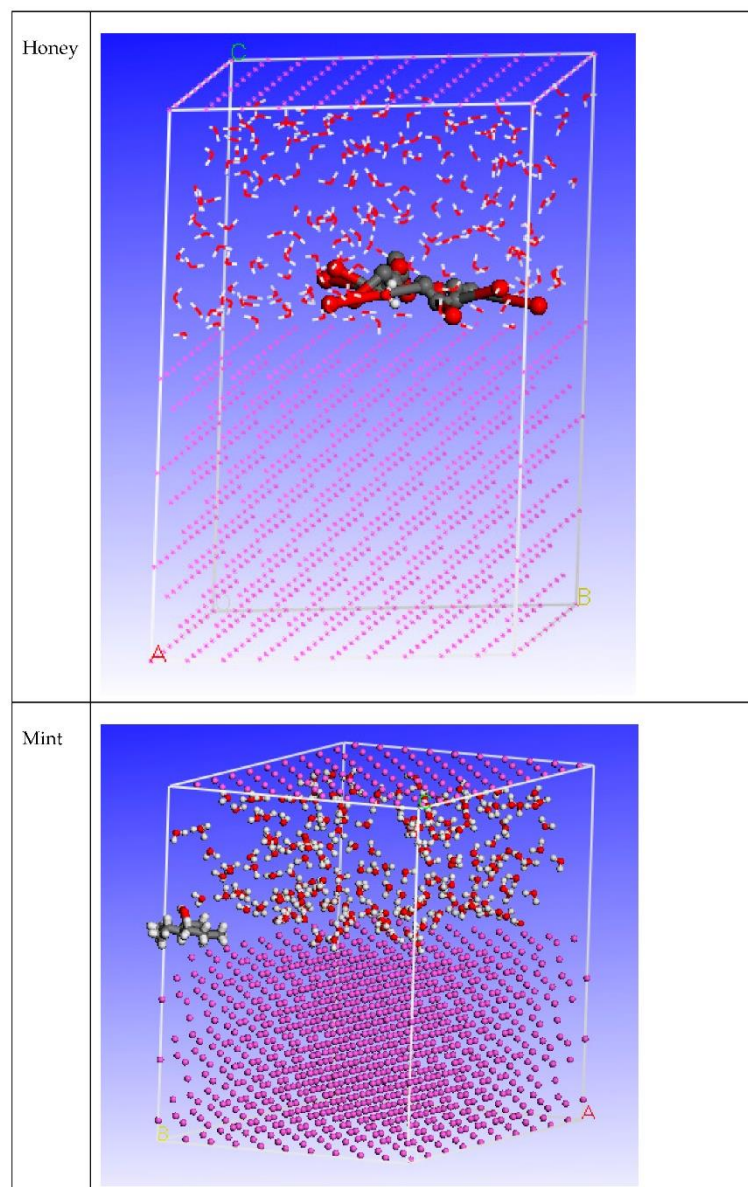


**Figure 4.** The adsorption locator module achieved the maximal suitable conformation for the adsorption of the synthesized hydrazides on the Al (1 1 1) substrate.

**Table 3.** Data and descriptors obtained using the Monte Carlo simulation for the adsorption of Honey and Mint compounds on Al (1 1 1) <sup>a</sup>.

Compound	Adsorption Energy	Rigid Adsorption Energy	Deformation Energy	Inhibitor: dEads/dNi	Water: dEads/dNi
Honey	−9570.46	−235.35	956.81	−289.75	−4.53
Mint	−9114.16	−228.31	911.18	−257.15	−4.53

<sup>a</sup> The dEads/dNi figures help to clarify the energy of the metal adsorbate arrangement when the energy of the adsorbates was ignored. Honey had a greater adsorption than Mint, as evidenced by the higher dEads/dNi values for Honey molecules (−9570.46 kcal mol<sup>−1</sup>) compared to −9114.16 kcal mol<sup>−1</sup>. In addition, the fact that water molecules have a dEads/dNi value of 4.53 kcal mol<sup>−1</sup> indicating that Honey and Mint have a larger affinity for adsorption than water. Thus, Honey and Mint created a solid protective barrier and were definitively adsorbed on the Al surface.

### 3.3. Outcomes of the Experiment

#### 3.3.1. Type of Inhibitor Effect

##### Gravimetric Calculations

Table 4 summarizes the data of the percentage IE and the surface coverage values ( $\theta$ ) that were obtained from using the weight loss method as the inhibitors at 900 ppm in 1 M HCl.

**Table 4.** Calculated values of (%IE) and ( $\theta$ ) by using the Weight Loss method for aluminum in the aqueous solution of inhibitor and 1 M HCl (duration is 2 h). The standard deviation is shown by the ( $\pm$ ) sign, and these numbers represent the average of three measurements.

Inhibitor	(%IE)	( $\theta$ )
Honey	89.3 ( $\pm$ ) 1.2	0.89
Mint	85.2 ( $\pm$ ) 0.95	0.85

The best inhibitor was Honey, as shown by the above results, and the percentage IE for the various studied substances decreased in the following order: Honey > Mint

The inhibitory effect of honey and mint was attributed to their compositions' adsorption on the aluminum surface. The presence of oxygen and electron donors from their double or aromatic bonds, which restricted the active sites on the metal, caused the corrosion rate to decrease, and the electron transfer value is the number of electrons transferred by organic compounds to the metal surface [57]. Honey has many hydroxyl groups which increase its electron-donating ability at the metal's surface when compared with that of mint (which has only one hydroxyl group); this explains the higher IE of honey than that of mint.

Inhibitor adsorption occurs on a metal's surface either physically or chemically. Some factors can facilitate the adsorption of organic inhibitors by metals such as the presence of molecules with empty, low-lying energy orbitals and molecules with electrons or hetero species, which are almost inaccessible due to their bonding with electron pairs. This will result in interactions between adsorbates that have unshared pairs of electrons with the surfaces of metals, and lead to form a coordinate type of the bonding system [58].

The type of the functional group in the organic corrosion inhibitors, and their structures, determine the bonding strength. Additionally, the presence of weakly bound electrons, such as those in neutral compounds and anions containing lone pairs of electrons, or in an electron system conjugated with aromatic rings or triple bonds, encourages electron transfer from the adsorbed inhibitor. It can happen when there are hetero species (e. g., O, S, N, P, and Se) in the adsorbed materials as well as lone-pair and/or aromatic units.

In addition, the hydroxyl groups in honey are more acidic, and the presence of a common ion effect and the absence of electron groups give rise to the H<sup>+</sup> effect. Because the presence of alkyl groups gives electron richness, the influence of H<sup>+</sup> is minimized in the mint condition.

##### Gasometry

Figure 5 illustrates the volume of evolved hydrogen versus the reaction time during the sample corrosion in 1 M HCl solutions in the presence and in the absence of various inhibitors. After a set amount of time from immersion of the aluminum in the test solution, the hydrogen evolution began. This duration is thought to correspond to the time the acid takes to degrade the pre-deposited inhibitor film before the metal assault begins, and it is known as the incubation period. According to available data, there is a linear relationship between the time of reaction and the volume of hydrogen evolved in all the examined solutions. On the other hand, the presence of the inhibitor decreases the straight line's slope significantly. The honey inhibitor has a strong capacity to prevent aluminum corrosion in acid solutions, based on the slope of the line, which represents the rate of corrosion. The IE

values and the surface coverage values ( $\theta$ ) of different inhibitors used in 1 M HCl generated from the H<sub>2</sub>-evolution technique are listed in Table 5.

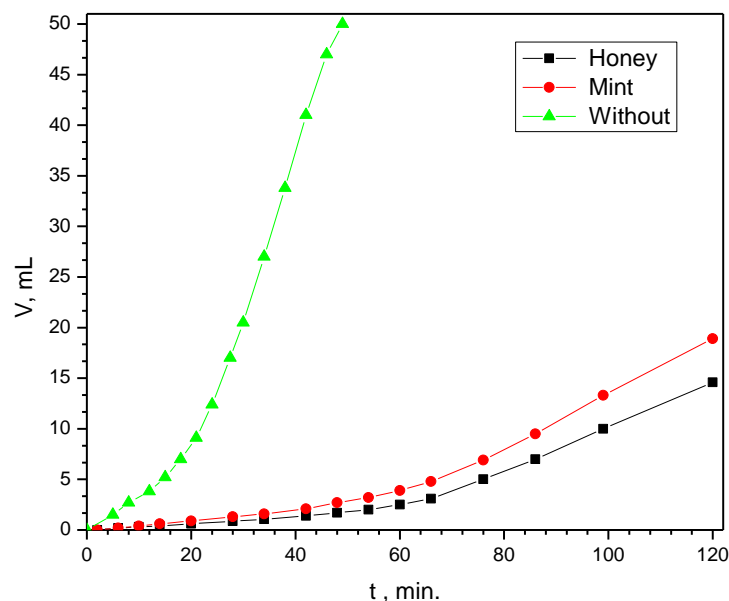


**Figure 5.** Hydrogen evolution during the Aluminum corrosion in 1 M HCl in the absence and the presence of 900 ppm of inhibitors.

**Table 5.** Percentage IE and surface coverage ( $\theta$ ) values acquired, using the hydrogen–evolution approach in the presence of the inhibitors in 1 M HCl. The standard deviation is shown by the ( $\pm$ ) sign, and these numbers represent the average of three measurements.

Inhibitor Type	(%IE)	( $\theta$ )
Honey	86 ( $\pm$ ) 0.81	0.86
Mint	82.1 ( $\pm$ ) 0.89	0.82

These data also show that honey was the best inhibitor, and the percentage IE for the various studied substances decreased in the following order: honey > mint.

### 3.3.2. Impact of Inhibitor Concentration

#### Gravimetry Method

The impact of inhibitor concentration via the weight loss approach was utilized to consider a honey inhibitor as an example. Table 6 summarizes the values of proportion IE and the fractional surface insurance values ( $\theta$ ) obtained by employing the weight loss technique for diverse concentrations of honey inhibitors in 1 M HCl.

**Table 6.** IE and fractional surface coverage values ( $\theta$ ) were gained using a weight loss technique for aluminum in an aqueous solution of 1 M HCl for two hours in the absence and presence of different concentrations of honey as the inhibitor. The standard deviation is shown by the ( $\pm$ ) sign, and these numbers represent the average of three measurements.

Inhibitor Concentration	(%IE)	( $\theta$ )
(900 ppm)	89.3 ( $\pm$ ) 0.43	0.89
(600 ppm)	62.5 ( $\pm$ ) 0.47	0.63
(450 ppm)	49.4 ( $\pm$ ) 0.72	0.49
(300 ppm)	38.1 ( $\pm$ ) 0.84	0.38

With an increment in the inhibitor's concentration, the weight loss diminished, and so the corrosion inhibition strengthened as can be seen in Table 5. This pattern might be explained by the fact that, as the concentration rises, so do adsorption and surface insurance. Hence, the surface and the medium are effectively separated.

### 3.3.3. Isotherm of Adsorption

Adsorption behaviour can be used to understand the mechanism of corrosion inhibition. The approach of fitting data to several isotherms was used to assess the data graphically. Figure 6 shows a plot of  $\log \theta$  vs.  $\log C$ , (Table 7), for the employed inhibitor, indicating that these compounds adsorb on the aluminum surface according to the Freundlich adsorption isotherm, which obeys the following relationship:

$$\log \theta = \log K + 1/n \log C \quad (n > 1)$$

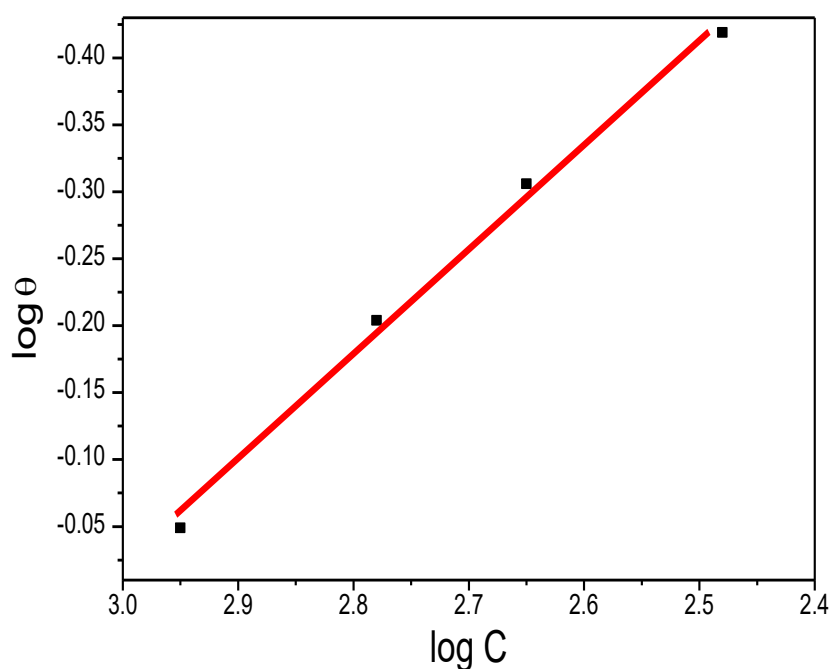


**Figure 6.** Freundlich adsorption isotherm curve fitting of corrosion data for aluminum in 1 M HCl in the presence of varying concentrations of honey inhibitor.

**Table 7.** Log C and Log ( $\theta$ ) values obtained from Table 5.

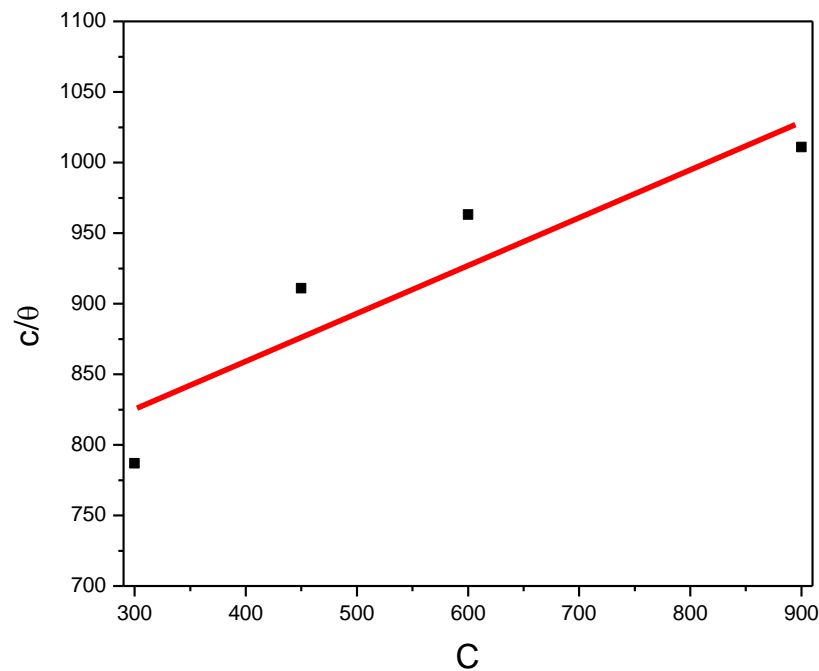
Log C	Log $\theta$
2.95	-0.049
2.78	-0.204
2.65	-0.306
2.48	-0.419

The findings showed that the Freundlich adsorption isotherm is valid for this inhibitor ( $R^2 = 0.99$ ), with a straight line of intercept  $\log K$  ( $K = 4.15 \times 10^{-3}$ ) and slope  $1/n$  ( $n = 1.27$ ).

On the aluminium surface, a plot of data in Table 8,  $(c/\theta)$  vs.  $c$ , for the employed inhibitor (Figure 7) indicates that the adsorption does not follow the Langmuir adsorption isotherm,  $R^2 = 0.7728$ .

**Table 8.**  $(c/\theta)$ ,  $(\theta)$ , and  $c$  values as determined from Table 5.

Inhibitor Concentration	$(\theta)$	$(c/\theta)$
(900 ppm)	0.89	1011
(600 ppm)	0.63	963
(450 ppm)	0.49	911
(300 ppm)	0.38	787

**Figure 7.** Fitting the Langmuir adsorption isotherm to the corrosion data for aluminium in 1 M HCl in the presence of varying amounts of the honey inhibitor.

### 3.4. Metal Surface SEM Analysis

Figure 8a,b shows a magnified ( $\times 2500$ ) SEM image of an aluminum specimen submerged in 1 M HCl for 1 h in the absence and presence of a honey inhibitor system. Figure 8a shows SEM micrographs of the aluminum surface in HCl without the inhibitor in which the roughness of the metal surface demonstrates aluminum corrosion in HCl.

Figure 8b shows that, when the honey inhibitor is present, the surface coverage rises, resulting in the production of the adsorbed compound on the metal's surface, which is then coated by a layer of inhibitor, thus controlling aluminum dissolution.

Finally, the importance of the inverse problem's solution for the best possible design of the experiments must be emphasized. Finding the ideal corrosion inhibitor concentration and immersion or exposure period really improves experiment control and enables a more accurate computation of the actual and fictitious impedances of aluminum in each solution. Even while making plans for future work, a closed-loop controller can be made by using the best values found for concentration and immersion or exposure time as process references [37,58].

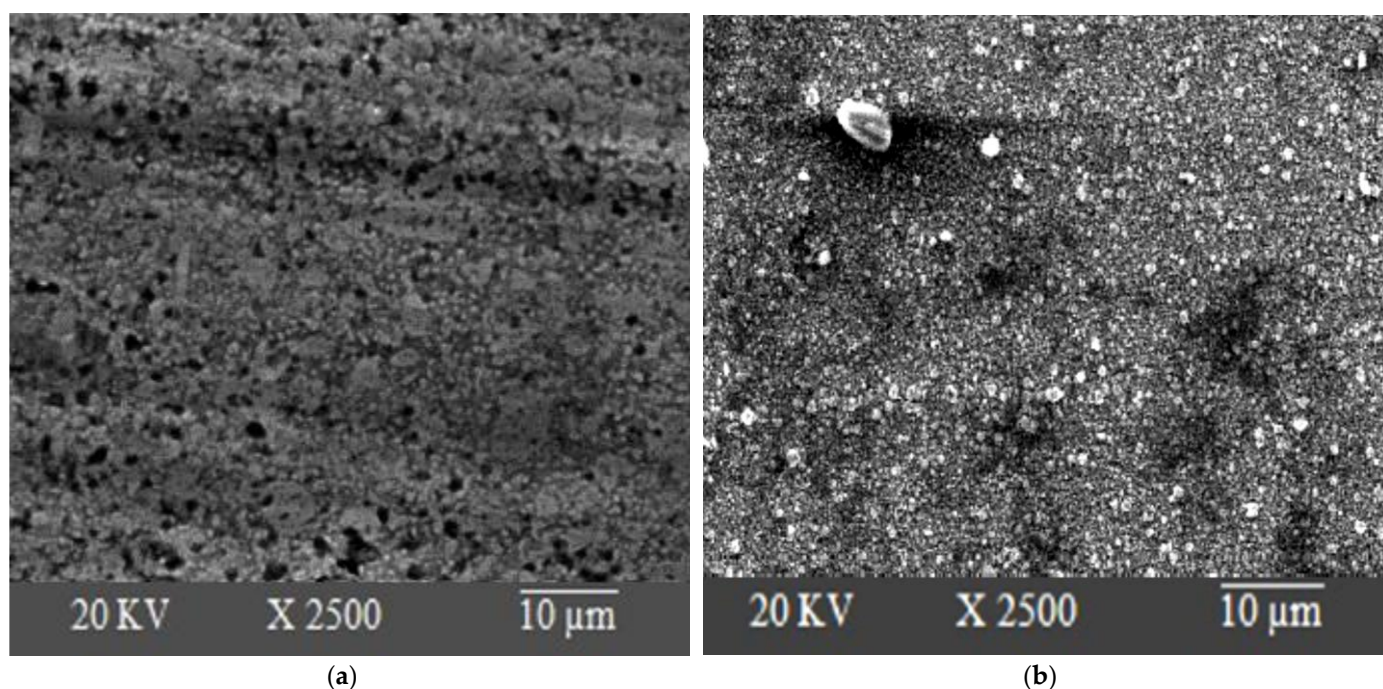


**Figure 8.** (a) SEM for pure aluminum in 1 M HCl in the absence of inhibitor; (b) SEM for pure aluminum in 1 M HCl in the presence of honey inhibitor.

#### 4. Conclusions

The reactivity parameters of honey and mint were investigated in terms of their respective IEs, using theoretical DFT simulations. Honey is highly capable as an effective surface coating for metal to prevent the latter against corrosion, according to all of the quantum chemical characteristics, describing the IE. The theoretical conclusions reached were in good agreement with the experimental findings. Honey and mint are both efficient corrosion inhibitors in HCl as can be understood from the results of several experiments, but honey is the best. Adsorption of organic materials on the metal's surface inhibited corrosion activity. By physically adhering to the corroding metallic surface, the inhibitors that were investigated successfully lowered the rate of aluminum corrosion in HCl. As the concentration of honey was increased, the efficacy of the inhibition also increased. It was concluded that the Freundlich adsorption isotherm governed the adsorption of honey on aluminum surfaces in 1 M HCl. The SEM images showed how the protection layer on the metal's surface was constructed. The gasometric calculations and those concerning weight loss IE were in reasonable agreement with each other.

**Author Contributions:** Conceptualization, T.A.Y. and M.M.A.-K.; methodology, T.A.Y. and M.M.A.-K.; soft-ware, T.A.Y. and R.K.H.; validation, T.A.Y., M.M.A.-K. and R.K.H.; formal analysis, R.K.H. and M.M.A.-K.; investigation, T.A.Y., M.M.A.-K., A.T.A.-E. and M.B.A.-O.; resources, T.A.Y.; data curation, R.K.H.; writing—original draft preparation, T.A.Y. and M.M.A.-K.; writing—review and editing, A.G.A. and R.K.H.; visualization, A.T.A.-E., M.B.A.-O. and T.A.Y.; supervision, M.M.A.-K.; project administration, A.G.A.; funding acquisition, A.G.A. All authors have read and agreed to the published version of the manuscript.

**Funding:** The authors extend their appreciation to the Deanship of Scientific Research at Imam Mohammad Ibn Saud Islamic University for funding this work through Research Group No. RG-21-09-79.

**Institutional Review Board Statement:** Not Applicable.

**Informed Consent Statement:** Not Applicable.

**Acknowledgments:** The authors extend their appreciation to the Deanship of Scientific Research at Imam Mohammad Ibn Saud Islamic University for funding this work through Research Group No. RG-21-09-79.

**Conflicts of Interest:** The authors declare no conflict of interest.

## References

1. Ennouri, A.; Lamiri, A.; Essahli, M. Corrosion Inhibition of Aluminium in Acidic Media by Different Extracts of *Trigonella foenum-graecum* L Seeds. *Port. Electrochim. Acta* **2017**, *35*, 279. [[CrossRef](#)]
2. El-Etre, A. Inhibition of aluminum corrosion using *Opuntia* extract. *Corros. Sci.* **2003**, *45*, 2485–2495. [[CrossRef](#)]
3. Muller, B. Corrosion inhibition of aluminium and zinc pigments by saccharides. *Corros. Sci.* **2002**, *44*, 1583–1591. [[CrossRef](#)]
4. Ryl, J.; Wysocka, J.; Cieslik, M.; Gerengi, H.; Ossowski, T.; Krakowiak, S.; Niedzialkowski, P. Understanding the origin of high corrosion inhibition efficiency of bee products towards aluminium alloys in alkaline environments. *Electrochim. Acta* **2019**, *304*, 263–274. [[CrossRef](#)]
5. Raghavendra, N.; Bhat, J.I. Anti-corrosion properties of areca palm leaf extract on aluminum in 0.5 M HCl. *S. Afr. J. Chem.* **2018**, *71*, 30–38. [[CrossRef](#)]
6. Chaubey, N.; Singh, V.K.; Quraishi, M.A. Electrochemical approach of Kalmegh leaf extract on the corrosion behavior of aluminium alloy in alkaline solution. *Int. J. Ind. Chem.* **2017**, *8*, 75–82. [[CrossRef](#)]
7. Oguzie, E.E. Corrosion inhibition of mild steel in hydrochloric acid solution by methylene blue dye. *Mater. Lett.* **2005**, *59*, 1076–1079. [[CrossRef](#)]
8. Oguzie, E.E. Inhibiting effect of crystal violet dye on aluminium corrosion in acidic and alkaline media. *Chem. Eng. Commun.* **2008**, *196*, 591–601. [[CrossRef](#)]
9. Oguzie, E.E.; Onuoha, G.N.; Onuchukwu, A.I. The inhibition of aluminium corrosion in potassium hydroxide by “Congo Red” dye, and synergistic action with halide ions. *Anti Corros. Methods. Mater.* **2005**, *52*, 293–298. [[CrossRef](#)]
10. Haley, T.J. Pharmacology and toxicology of the rare earth elements. *J. Pharm. Sci.* **1965**, *54*, 663–670. [[CrossRef](#)]
11. Bethencourt, M.; Botana, F.J.; Calvino, J.J.; Marcos, M.; Rodriguez-Chacon, M.A. Lanthanide compounds as environmentally-friendly corrosion inhibitors of aluminium alloys: A review. *Corros. Sci.* **1998**, *40*, 1803–1823. [[CrossRef](#)]
12. Ju, H.; Kai, Z.P.; Li, Y. Aminic nitrogen-bearing polydentate Schiff base compounds as corrosion inhibitors for iron in acidic media: A quantum chemical calculation. *Corros. Sci.* **2008**, *50*, 865–871. [[CrossRef](#)]
13. Ahamad, I.; Prasad, R.; Quraishi, M.A. Thermodynamic, electrochemical and quantum chemical investigation of some Schiff bases as corrosion inhibitors for mild steel in hydrochloric acid solutions. *Corros. Sci.* **2010**, *52*, 933–942. [[CrossRef](#)]
14. Solmaz, R.; Altunbas, E.; Kardas, G. Adsorption and corrosion inhibition effect of 2-((5-mercapto-1,3,4-thiadiazol-2-ylimino)methyl)phenol Schiff base on mild steel. *Mater. Chem. Phys.* **2011**, *125*, 796–801. [[CrossRef](#)]
15. El-Naggar, M.M. Corrosion inhibition of mild steel in acidic medium by some sulfa drugs compounds. *Corros. Sci.* **2007**, *49*, 2226–2236. [[CrossRef](#)]
16. Gece, G. Drugs: A review of promising novel corrosion inhibitors. *Corros. Sci.* **2011**, *53*, 3873–3898. [[CrossRef](#)]
17. Xhanari, K.; Finsgar, M.; Knez Hrnčić, M.; Maver, U.; Knez, Z.; Seiti, B. Green corrosion inhibitors for aluminium and its alloys: A review. *RSC Adv.* **2017**, *7*, 27299–27330. [[CrossRef](#)]
18. Mansfeld, F. *Corrosion Mechanisms*, 1st ed.; CRC Press: Boca Raton, FL, USA, 1987; pp. 157–170. [[CrossRef](#)]
19. Rosliza, R.; Wan Nik, W.B.; Izman, S.; Prawoto, Y. Anti-corrosive properties of natural honey on AlMgSi alloy in seawater. *Curr. Appl. Phys.* **2010**, *10*, 923–929. [[CrossRef](#)]
20. Gudic, S.; Vrsalovic, L.; Kliskic, M.; Jerkovic, I.; Radonic, A.; Zekic, M. Corrosion inhibition of AA 5052 aluminium alloy in NaCl solution by different types of honey. *Int. J. Electrochem. Sci.* **2016**, *11*, 998–1011.
21. Rahim, A.A.; Rocca, E.; Steinmetz, J.; Kassim, M.J. Inhibitive Action of Mangrove Tannins and Phosphoric Acid on Pre-Rusted Steel via Electrochemical Methods. *Corros. Sci.* **2008**, *50*, 1546–1550. [[CrossRef](#)]
22. Rahim, A.A.; Kassim, J. Recent development of vegetal tannins in corrosion protection of iron and steel. *Recent Pat. Mater. Sci.* **2008**, *1*, 223–231. [[CrossRef](#)]
23. Shah, A.M.; Rahim, A.A.; Yahya, S.; Raja, P.B.; Hamid, S.A. Acid corrosion inhibition of copper by mangrove tannin. *Pigm. Resin Technol.* **2011**, *40*, 118–122. [[CrossRef](#)]
24. Raja, P.B.; Sethuraman, M.G. Natural Products as Corrosion Inhibitor for Metals in Corrosive Media: A Review. *Mater. Lett.* **2008**, *62*, 113–116. [[CrossRef](#)]
25. Bedair, M.A.; Metwally, M.S.; Soliman, S.A.; Al-Sabagh, A.M.; Salem, A.M.; Mohamed, T.A. Extracts of Mint and Tea as Green Corrosion Inhibitors for Mild Steel in Hydrochloric acid solution. *Al Azhar Bul. Sci.* **2015**, *26*, 1–14. [[CrossRef](#)]
26. El-Etre, A.Y.; Abdallah, M.; El-Tantawy, Z.E. Corrosion Inhibition of Some Metals Using Lawsonia Extract. *Corros. Sci.* **2005**, *47*, 385–395. [[CrossRef](#)]
27. Noor, E.A. Potential of Aqueous Extract of Hibiscus sabdariffa Leaves for Inhibiting the Corrosion of Aluminum in alkaline Solutions. *J. Appl. Electrochem.* **2009**, *39*, 1465–1475. [[CrossRef](#)]
28. Okafor, P.C.; Ebenso, E.E.; Ekpe, U.J. Azadirachta indica Extracts as Corrosion Inhibitor for Mild Steel in Acid Medium. *Int. J. Electrochem. Sci.* **2010**, *5*, 978–993.

29. Hassan, A.T.; Hussein, R.K.; Abou-krissha, M.; Attia, M.I. Density Functional Theory Investigation of Some Pyridine Dicarboxylic Acids Derivatives as Corrosion Inhibitors. *Int. J. Electrochem. Sci.* **2020**, *15*, 4274–4286. [[CrossRef](#)]
30. Hussein, R.K.; Abou-Krissha, M.; Yousef, T.A. Theoretical and Experimental Studies of Different Amine Compounds as Corrosion Inhibitors for Aluminum in Hydrochloric Acid. *Biointerface Res. Appl. Chem.* **2021**, *11*, 9772–9785.
31. Musa, A.Y.; Kadhum, A.A.; Mohamad, A.B.; Takriff, M.S.; Kamarudin, S.K. On the inhibition of mild steel corrosion by 4-amino-5-phenyl-4H-1, 2, 4-triazole-3- thiol. *Corros. Sci.* **2010**, *52*, 526–533. [[CrossRef](#)]
32. *HyperChem Version 8.0*; Hypercube, Inc.: Waterloo, ON, Canada, 2002.
33. Zhang, X.Y.; Kang, Q.X.; Wang, Y. Theoretical study of N-thiazolyl-2-cyanoacetamide derivatives as corrosion inhibitor for aluminum in alkaline environments. *Comput. Theor. Chem.* **2018**, *1131*, 25–32. [[CrossRef](#)]
34. Sun, H. COMPASS: An ab initio force-field optimized for condensed-phase applications—Overview with details on alkane and benzene compounds. *J. Phys. Chem. B* **1998**, *102*, 7338–7364. [[CrossRef](#)]
35. Kasuga, B.; Park, E.; Machunda, R.L. Inhibition of Aluminium Corrosion Using *Carica papaya* Leaves Extract in Sulphuric Acid. *J. Miner. Mater. Character. Eng.* **2018**, *6*, 1–14. [[CrossRef](#)]
36. HZhang, H.; Chen, Y. Experimental and theoretical studies of benzaldehyde thiosemicarbazone derivatives as corrosion inhibitors for mild steel in acid media. *J. Mol. Struct.* **2019**, *1177*, 90–100. [[CrossRef](#)]
37. El-Saeed, H.M.; Fouda, A.S.; Deyab, M.A.; Shalabi, K.; Nessim, M.I.; El-Katori, E.E. Synthesis and characterization of novel ionic liquids based on imidazolium for acid corrosion inhibition of aluminum: Experimental, spectral, and computational study. *J. Mol. Liq.* **2022**, *358*, 119177. [[CrossRef](#)]
38. Edoziuno, F.O.; Adediran, A.A.; Odoni, B.U.; Akinwekomi, A.D.; Adesina, O.S.; Oki, M. Optimization and development of predictive models for the corrosion inhibition of mild steel in sulphuric acid by methyl-5-benzoyl-2-benzimidazole carbamate (mebendazole). *Cogent Eng.* **2020**, *7*, 1714100. [[CrossRef](#)]
39. Ebenso, E.E.; Verma, C.; Olasunkanmi, L.O.; Akpan, E.D.; Verma, D.K.; Lgaz, H.; Guo, L.; Kaya, S.; Quraishi, M.A. Molecular modelling of compounds used for corrosion inhibition studies: A review. *Phys. Chem. Chem. Phys.* **2021**, *36*, 19987–20027. [[CrossRef](#)]
40. Zheng, X.W.; Zhang, S.T.; Li, W.P.; Yin, L.L.; He, J.H.; Wu, J.F. Investigation of 1-butyl-3-methyl-1H-benzimidazolium iodide as inhibitor for mild steel in sulfuric acid solution. *Corros. Sci.* **2014**, *80*, 383–392. [[CrossRef](#)]
41. Cao, Z.Y.; Tang, Y.M.; Cang, H.; Xu, J.Q.; Lu, G.; Jing, W.H. Novel benzimidazole derivatives as corrosion inhibitors of mild steel in the acidic media. Part II: Theoretical studies. *Corros. Sci.* **2014**, *83*, 292–298. [[CrossRef](#)]
42. Gece, G. The use of quantum chemical methods in corrosion inhibitor studies. *Corros. Sci.* **2008**, *50*, 2981–2992. [[CrossRef](#)]
43. Sayin, K.; Karakas, D. Quantum chemical studies on the some inorganic corrosion inhibitors. *Corros. Sci.* **2013**, *77*, 37–43. [[CrossRef](#)]
44. Mourya, P.; Singh, P.; Tewari, A.K.; Rastogi, R.B.; Singh, M.M. Relationship between structure and inhibition behaviour of quinolinium salts for mildsteel corrosion: Experimental and theoretical approach. *Corros. Sci.* **2015**, *95*, 71–78. [[CrossRef](#)]
45. Kosari, A.; Moayed, M.H.; Davoodi, A.; Parvizi, R.; Momeni, M.; Eshghi, H.; Moradi, H. Electrochemical and quantum chemical assessment of two organic compounds from pyridine derivatives as corrosion inhibitors for mild steel in HCl solution under stagnant condition and hydrodynamic flow. *Corros. Sci.* **2014**, *78*, 138–145. [[CrossRef](#)]
46. Obi-Egbedi, N.O.; Obot, I.B. Inhibitive properties, thermodynamic and quantum chemical studies of alloxazine on mild steel corrosion in H<sub>2</sub>SO<sub>4</sub>. *Corros. Sci.* **2011**, *53*, 263–278. [[CrossRef](#)]
47. Behpour, M.; Ghoreishi, S.M.; Khayatkashani, M.; Soltani, N. The effect of two oleo-gum resin exudate from *Ferula assa-foetida* and *Dorema ammoniacum* on mild steel corrosion in acidic media. *Corros. Sci.* **2011**, *53*, 2489–2501. [[CrossRef](#)]
48. Khaled, K.F.; Babic-Samardzija, K.; Hackerman, N. Theoretical study of the structural effects of polymethylene amines on corrosion inhibition of iron in acid solutions. *Electrochim. Acta* **2005**, *50*, 2515–2520. [[CrossRef](#)]
49. Khalil, N. Quantum chemical approach of corrosion inhibition. *Electrochim. Acta* **2003**, *48*, 2635–2640. [[CrossRef](#)]
50. Qurashi, M.A.; Sardar, R. Hector bases-a new class of heterocyclic corrosion inhibitors for mild steel in acid solutions. *J. Appl. Electrochem.* **2003**, *33*, 163–169. [[CrossRef](#)]
51. Zarrouk, A.; Hammouti, B.; Lakhlifi, T.; Traisnel, M.; Vezin, H.; Bentiss, F. New 1Hpyrrole-2, 5-dione derivatives as efficient organic inhibitors of carbon steel corrosion in hydrochloric acid medium: Electrochemical, XPS and DFT studies. *Corros. Sci.* **2015**, *90*, 572–584. [[CrossRef](#)]
52. Karelson, M.; Lobanov, V.S. Quantum-Chemical Descriptors in QSAR/QSPR Studies. *Chem. Rev.* **1996**, *96*, 1027–1044. [[CrossRef](#)]
53. Cherry, W.; Epiotis, N.; Borden, W.T. Effect of filled “pi” and unfilled “sigma” molecular orbital interactions on molecular structure. *Acc. Chem. Res.* **1977**, *10*, 167–173. [[CrossRef](#)]
54. Bereket, G.; Öğretir, C.; Yurt, A. Quantum mechanical calculations on some 4-methyl-5-substituted imidazole derivatives as acidic corrosion inhibitor for zinc. *J. Mol. Struct. THEOCHEM* **2001**, *571*, 139–145. [[CrossRef](#)]
55. Yadav, M.; Kumar, S.; Sinha, R.R.; Bahadur, I.; Ebenso, E.E. New pyrimidine derivatives as efficient organic inhibitors on mild steel corrosion in acidic medium: Electrochemical, SEM, EDX, AFM and DFT studies. *J. Mol. Liqui.* **2015**, *211*, 135–145. [[CrossRef](#)]
56. Sasikumar, Y.; Adekunle, A.S.; Olasunkanmi, L.O.; Bahadur, I.; Baskar, R.; Kabanda, M.M.; Obot, I.B.; Ebenso, E.E. Experimental, quantum chemical and Monte Carlo simulation studies on the corrosion inhibition of some alkyl imidazolium ionic liquids containing tetrafluoroborate anion on mild steel in acidic medium. *J. Mol. Liq.* **2015**, *211*, 105–118. [[CrossRef](#)]

- 
57. Sherif, E.M.; Park, S.M. Effects of 1,4-naphthoquinone on aluminum corrosion in 0.50 m sodium chloride solutions. *Electrochim. Acta* **2006**, *51*, 1313–1321. [[CrossRef](#)]
  58. Méndez-Figueroa, G.H.; Ossandón, S.; Fernández, J.A.R.; Martínez, R.G.; Vázquez, A.E.; Orozco-Cruz, R. Electrochemical evaluation of an *Acanthocereus tetragonus* aqueous extract on aluminum in NaCl (0.6 M) and HCl (1 M) and its modelling using forward and inverse artificial neural networks. *J. Electroanal. Chem.* **2022**, *918*, 116444. [[CrossRef](#)]